## First steps with HLLMHD and PP reconstruction: Part V

by *O. Steiner*

Part V revisits part II of the present report. We repeat calculations with the same solar and stellar models (obtained from Matthias Steffen), using the CO5BOLD-code version `for_2012.11.05f` instead of version `for_2011.04.28` that was used in parts I-III. Version f is a further development of version b that was used in part IV. We mainly ran the model `d3t50g45mm00n04` with $T_{\rm eff} = 5000$ K and $\log g = 4.5$ (compared to 5770 and 4.44 for the Sun). This model has n1 $\times$ n2 $\times$ n3 $= 140 \times 140 \times 141$ grid cells; the size of the box is 4.942 Mm $\times$ 4.942 Mm $\times$ 2.483871 Mm. The $\tau = 1$ level is at a height of about 1.76 Mm from the bottom ($\approx 724$ km from the top). The grid cells have an equidistant horizontal width of 35.3 km and a non-equidistant vertical size, varying from 66.3 km in the bottom part of the box to $\approx 12$ km near $\tau = 1$, down to 7.38 km in the top part of the box. The initial model consists of relaxed convection as computed with the Roe solver and the Van Leer reconstruction scheme. The initial magnetic field (if not set zero or absent) is homogeneous and vertical with a strength of 50 G.

| job | solver | reconstr. | $\nu_{\rm Smag.}$ | $\nu_{\rm art.}$ | $B_{\rm init}$ [G] | initial model | $t_{\rm end}$ [s] |
|---|---|---|---|---|---|---|---|
| job_d3gt57g44n59_f | Roe | VanLeer | 0.0 | 0.0 | — | d3gt57g45n59.0384735 | 7202 |
| job_d3gt57g44n59_B0_f | HLLMHD | FRweno | 0.0 | 0.0 | $B_z = 0$ | d3gt57g45n59.0384735_B0 | 7202 |
| job_d3t50g45mm00n04_Roe_f/ | | | | | | | |
| vl | Roe | VanLeer | 0.0 | 0.0 | — | d3t50g45mm00n04.1079820 | 7202 |
| job_d3t50g45mm00n04_f/ | | | | | | | |
| FRweno | HLLMHD | FRweno | 0.0 | 0.0 | $B_z = 0$ | d3t50g45mm00n04_B0_1step | 48007 |
| PP | HLLMHD | PP | 0.0 | 0.0 | $B_z = 0$ | d3t50g45mm00n04_B0_1step | 7201 |
| PP_vissmag | HLLMHD | PP | 1.0 | 0.0 | $B_z = 0$ | d3t50g45mm00n04_B0_1step | 7201 |
| vl | HLLMHD | VanLeer | 0.0 | 0.0 | $B_z = 0$ | d3t50g45mm00n04_B0_1step | 7202 |
| job_d3t50g45mm00n04_v50_f/ | | | | | | | |
| FRweno | HLLMHD | FRweno | 0.0 | 0.0 | $B_z = 50$ | d3t50g45mm00n04_v50 | 37398 |
| PP | HLLMHD | PP | 0.0 | 0.0 | $B_z = 50$ | d3t50g45mm00n04_v50 | 7200 |
| vl | HLLMHD | VanLeer | 0.0 | 0.0 | $B_z = 50$ | d3t50g45mm00n04_v50 | 7200 |
| job_d3t40g45mm00n01_B0_f/ | | | | | | | |
| PP | HLLMHD | PP | 0.0 | 0.0 | $B_z = 0$ | d3t40g45mm00n01.1320402_B0 | 48008 |
| FRweno | HLLMHD | FRweno | 0.0 | 0.0 | $B_z = 0$ | d3t40g45mm00n01.1320402_B0 | 48008 |
| FRweno_radc | HLLMHD | FRweno | 0.0 | 0.0 | $B_z = 0$ | d3t40g45mm00n01.1320402_B0 | 48005 |
| FRweno_p2p | HLLMHD | FRweno | 0.0 | 0.0 | $B_z = 0$ | d3t40g45mm00n01.1320402_B0 | 48008 |
| job_d3t40g45mm00n01_Roe_f/ | | | | | | | |
| FRweno | Roe | FRweno | 0.0 | 0.0 | $B_z = 0$ | d3t40g45mm00n01.1320402_B0 | 48011 |

Table 1: Simulation runs carried out for part V. For job_d3t40g45mm00n01_B0_f/FRweno_radc, the Courant numbers for the radiation transfer were set C_radCourant = 0.8 and C_radCourantmax = 1.0, while these values were 2.4 and 2.6, respectively, for all other runs. For run job_d3t40g45mm00n01_B0_f/FRweno_p2p, the p2p viscosity was set c_visp2pcoeff = 0.2 and c_visp2phypsmagorinsky = 0.2. These values were zero for all other runs.

We also ran the model `d3t40g45mm00n01` with $T_{\rm eff} = 4000$ K and $\log g = 4.5$. This model too has n1 $\times$ n2 $\times$ n3 $= 140 \times 140 \times 141$ grid cells; the size of the box is 4.736 Mm $\times$ 4.736 Mm $\times$ 1.236155 Mm. The $\tau = 1$ level is at a height of about 0.74 Mm from the bottom ($\approx 496$ km from the top). The grid cells have an equidistant horizontal width of 33.8276 km and a non-equidistant vertical size, varying from 11.75 km in the bottom part of the box to $\approx 8$ km near $\tau = 1$, down to 6.78 km

in the top part of the box, which leaves the cells rather flat in this case. The initial model consists of relaxed convection as computed with the Roe solver and the Van Leer reconstruction scheme. The initial magnetic field (if not set zero or absent) is homogeneous and vertical with a strength of 50 G.

Finally, there is the solar model, `d3gt57g44n59`, with $T_{\rm eff} = 5770$ K and $\log g = 4.44$. This model has $\mathrm{n1} \times \mathrm{n2} \times \mathrm{n3} = 140 \times 140 \times 150$ grid cells; the size of the box is 5.6 Mm $\times$ 5.6 Mm $\times$ 2.2689 Mm. The $\tau = 1$ level is at a height of about 1.372 Mm from the bottom ($\approx$ 897 km from the top). The grid cells have an equidistant horizontal width of 40 km and an equidistant vertical size of 15.1261 km. The initial model consists of relaxed convection as computed with the Roe solver and the Van Leer reconstruction scheme. The initial magnetic field (if not set zero or absent) is homogeneous and vertical with a strength of 50 G.

Table 1 gives a compilation of all the models that were run for part V of this report, now with the code version `for_2012.11.05f`.

### Mass fluxes

One important result from part II of this report was that the Hancock time integration scheme produces spurious oscillations when applied to magnetic field-free cooler than solar models. In part III it was demonstrated that this problem could be remedied by either keeping the time steps short enough or by switching to a higher order Runge Kutta time integration scheme. The oscillations were best seen in the horizontally averaged mass flux at the height where $\tau = 1$ but they had most disastrous consequences for the bolometric intensity of the models. Here, we start examining the mass fluxes as a function of time, before turning to the bolometric intensity later on.

Figure 1 shows the horizontally averaged, vertical mass flux at the level of $\langle\tau\rangle = 1$ as a function of time for the stellar model `job_d3t50g45mm00n04`, once computed with the old code version `for_2011.04.28` (blue), and once with the new code version `for_2012.11.05f` (red). For both runs, the models had $\mathbf{B} = 0$ and were computed with the HLLMHD scheme and PP reconstruction. Clearly, with the new code version, the amplitude of the mass-flux oscillation is much smaller than with the old code version and it does not produce the double peaks as did the old version. These double peaks apparently caused the flickering in the bolometric intensity of the old model so that we can expect the intensity of the new model to behave normal as well. The time steps in the old model varied between about 0.15 s and 0.45 s. With the new code version, it stays more closely around 0.3 s. One difference between the two runs is, that the old model was computed with a Smagorinsky viscosity of $\nu_{\rm Smag.} = 1.0$ whereas for the new run, this parameter was set to zero. Another run with the new code version and with $\nu_{\rm Smag.} = 1.0$, however, revealed a similar oscillatory behavior like the run with $\nu_{\rm Smag.} = 0.0$: the amplitudes were even a bit smaller and the oscillations of the two runs were often out of phase but had similar frequency.

Figure 2 shows the horizontally averaged, vertical mass flux at the level of $\langle\tau\rangle = 1$ for the same $T_{\rm eff} = 5000$ K model as considered in Fig. 1, all computed with the new code version `for_2012.11.05f`. The three curves refer to three different numerical schemes. The blue curve results when using the Roe solver in combination with the

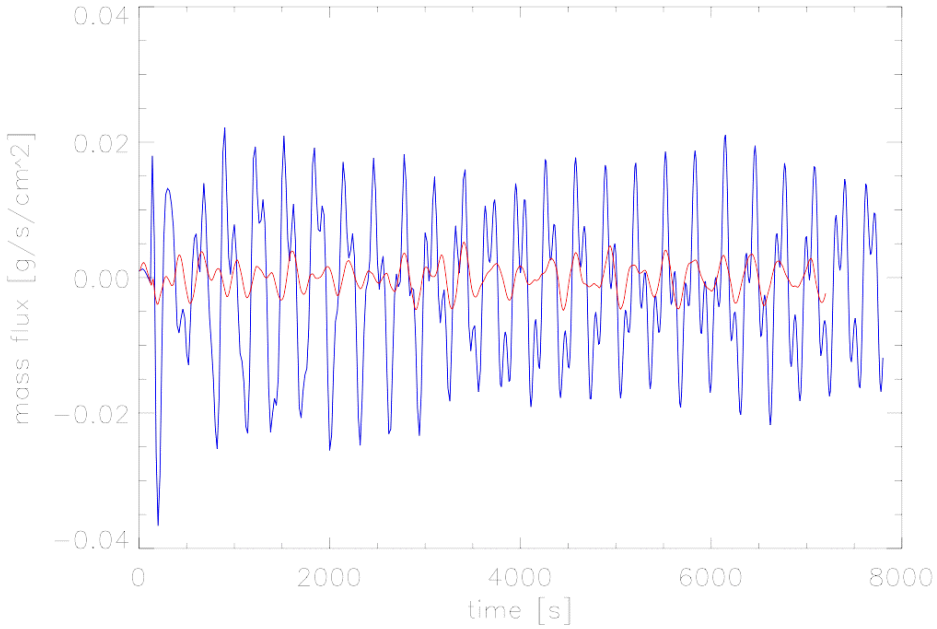


Figure 1: Horizontally averaged, vertical mass flux at the level of $\langle\tau\rangle = 1$ as a function of time for the stellar model with $T_{\rm eff} = 5000$ K and $\mathbf{B} = 0$, computed with HLLMHD and PP, once with the code version for_2011.04.28 (*blue*) and once with the code version for_2012.11.05f (*red*).

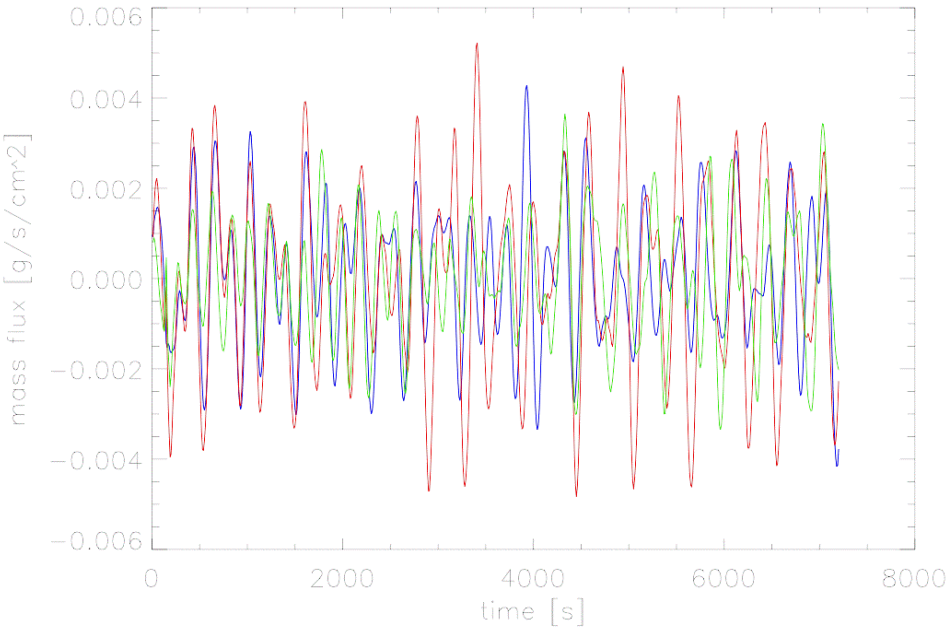


Figure 2: Horizontally averaged, vertical mass flux at the level of $\langle\tau\rangle = 1$ as a function of time for the stellar model with $T_{\rm eff} = 5000$ K with no magnetic field or $\mathbf{B} = 0$, computed with Roe+VanLeer (*blue*), HLLMHD+PP (*red*), and HLLMHD+FRweno (*green*). All models with the new code version for_2012.11.05f. Note that the scale of the abscissa is an order of magnitude smaller than in Fig. 1.

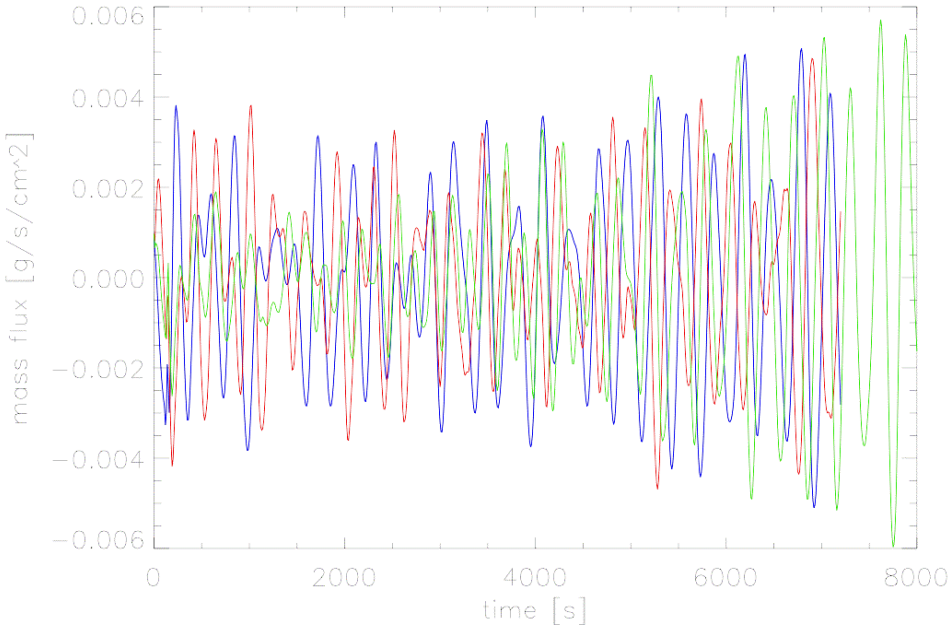


Figure 3: Horizontally averaged, vertical mass flux at the level of $\langle\tau\rangle = 1$ as a function of time for the stellar model with $T_{\rm eff} = 5000$ K and an initial vertical, homogeneous magnetic field of 50 G, computed with VanLeer (*blue*), PP (*red*), and FRweno (*green*). All models with the new code version for_2012.11.05f and HLLMHD.

VanLeer reconstruction scheme (the canonical combination used in the past, which we trust best), the red curve, when using HLLMHD and PP reconstruction, and the green curve with HLLMHD plus FRweno. Amplitude and frequency of the three methods are quite similar and an order of magnitude smaller than with the old code version. PP, being the least diffusive method, produces, as expected, the largest amplitudes.

We keep considering model `d3t50g45mm00n04` with $T_{\rm eff} = 5000$ K but introduce an initial homogeneous vertical magnetic field of strength 50 G. In part II of this report, we found that the spurious oscillations disappeared with the introduction of a magnetic field, because of the reduction of the time step that came with the introduction of the magnetic field. Thus, we expect no problems to occur here but still need to test if this was indeed the case. In fact, Fig. 3 meets our expectations. All three curves were obtained with `for_2012.11.05f` using the Hancock time integration scheme but different reconstructions: VanLeer (blue), PP (red), and FRweno (green). Again, the amplitude is of the order 0.004 g s$^{-1}$ cm$^{-2}$.

From Fig. 3, we can see that the amplitude of the oscillation in the run with FRweno increases with time. In fact, all curves seem to show this behavior. Therefore, we continued the FRweno run to see if the amplitude keeps increasing. This is in deed the case, as can be seen from Fig. 4 and it finally led to a crash of the simulation at time $t = 37\,398$ s. There is an amplitude modulation over a time span of the order 5000 s. This is in the order of the convective time scale: with $v_{\rm conv} \approx 0.5$ km/s near the bottom of the computational domain, it takes about 2000 s for a length scale of

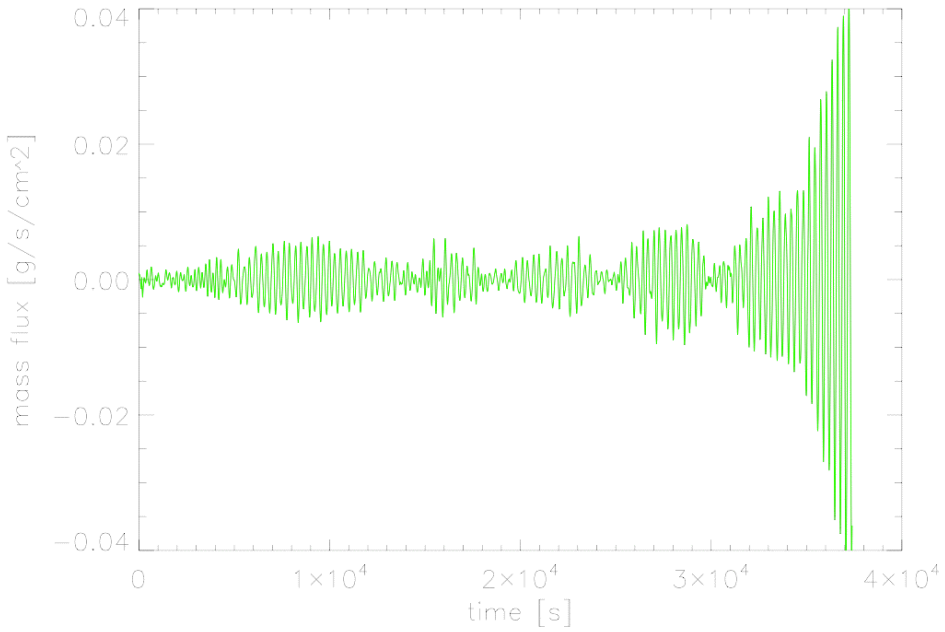


Figure 4: Horizontally averaged, vertical mass flux at the level of $\langle\tau\rangle = 1$ as a function of time for the stellar model with $T_{\rm eff} = 5000$ K and initial vertical magnetic field of 50 G, computed with the code version for_2012.11.05f using the HLLMHD solver and FRweno reconstruction. Crash at time $t = 37398$ s.

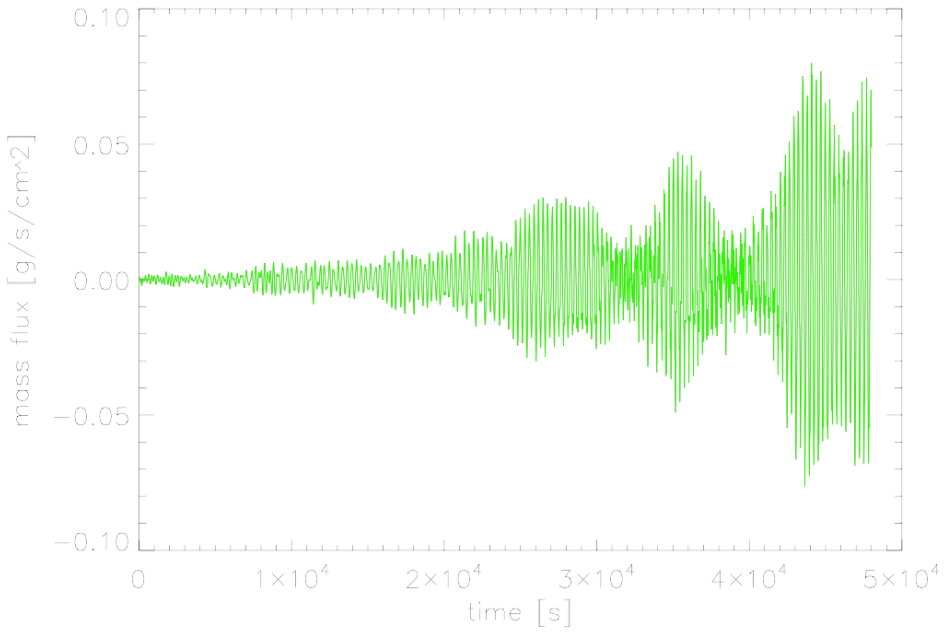


Figure 5: Horizontally averaged, vertical mass flux at the level of $\langle\tau\rangle = 1$ as a function of time for the stellar model with $T_{\rm eff} = 5000$ K and $\mathbf{B} = 0$ computed with the code version for_2012.11.05f using the HLLMHD solver and FRweno reconstruction. Note the difference in the mass-flux scale in comparison with Fig. 4.

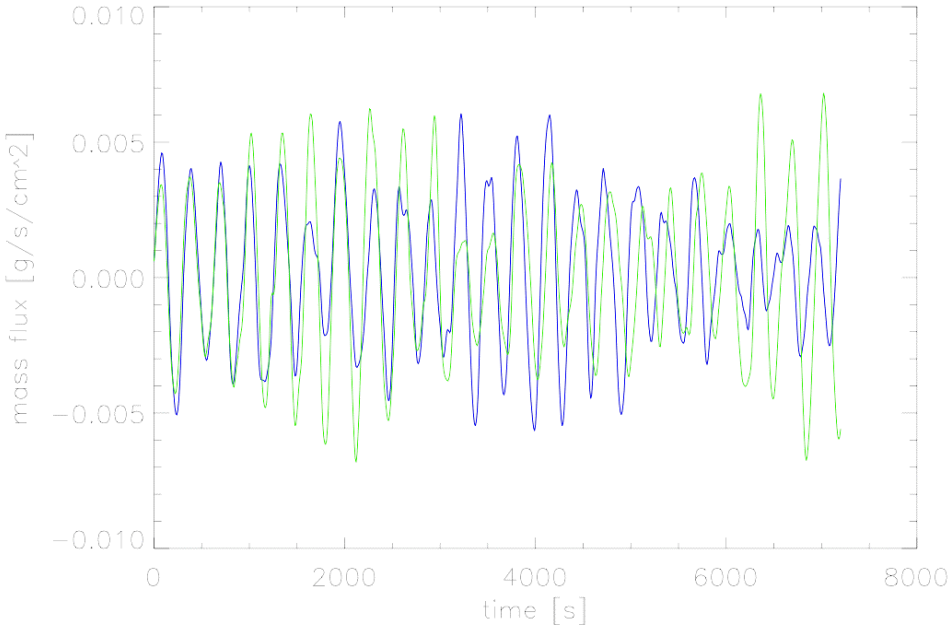


Figure 6: Horizontally averaged, vertical mass flux at the level of $\langle\tau\rangle = 1$ as a function of time for the solar model d3gt57g44n59. *Blue curve*: Magnetic field-free model advanced with the Roes solver and VanLeer reconstruction. *Green curve*: Model with $\mathbf{B} = 0$ advanced with the HLLMHD solver and FRweno reconstruction.

1 Mm. The amplitude growth is even more drastic for the model with $\mathbf{B} = 0$ as can be seen from Fig. 5 but this run did the entire requested time span of 48 007 s. The origin of this growth of the oscillation amplitude of the mass flux is not known at this point. It is a very slowly growing instability, which seems to be there from the beginning. It may become necessary to introduce a drag force or a viscosity in order to remedy this problem.

Finally, for comparison, we also show the mass flux through the $\langle\tau\rangle = 1$ level as a function of time for the solar model `d3gt57g44n59` on Fig. 6. There, the blue curve was obtained with the magnetic field-free model using the Roe solver and VanLeer reconstruction, the green curve with the HLLMHD solver and FRweno reconstruction, where we had $\mathbf{B} = 0$. Despite the fact that two employed methods are quite dissimilar, the two curves are quite similar with respect to amplitude and phase, which gives some confidence in the solution. The amplitude is of similar size as for the $T_{\rm eff} = 5000$ K model. The mean period is roughly 313 s corresponding to 3.2 mHz. For the $T_{\rm eff} = 5000$ K model, the corresponding approximate values are 256 s and 3.9 mHz, respectively.

**Radiative flux at the top boundary**

We now turn our attention to the oscillation of the radiative output. In part II of this report, we found very large oscillation amplitudes and a doubling of the frequency when computing with the Hancock time integration scheme, PP reconstruction, and the HLLMHD scheme. From the previous results, regarding the mass fluxes, we

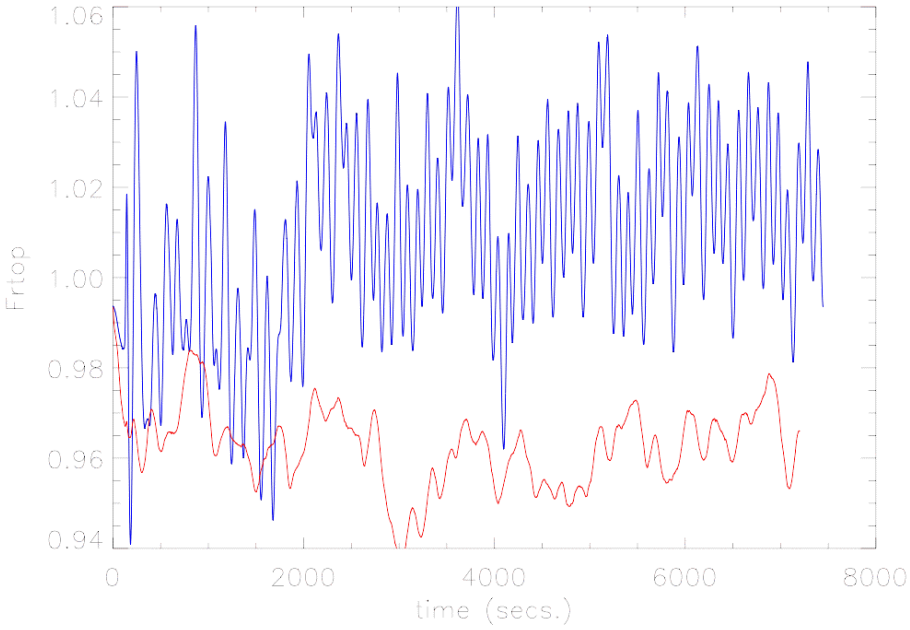


Figure 7: Bolometric radiative flux through the top boundary, Frtop, in units of $\sigma T_{\rm eff}^4$ as a function of time for model d3t50g45mm00n04 with $T_{\rm eff} = 5000$ K and $\mathbf{B} = 0$. *Blue:* Old run with code version for_2011.04.28. *Red:* New code version for_2012.11.05f. Both runs with HLLMHD+PP and Hancock time integration.

expect that this problem has disappeared with the new version. Figure 7 shows the total radiative output at the top in units of $\sigma T_{\rm eff}^4$ for the model `d3t50g45mm00n04` with $T_{\rm eff} = 5000$ K and $\mathbf{B} = 0$. Both curves were computed with Hancock time integration, the HLLMHD scheme, and PP reconstruction. The blue curve was obtained with the old code version `for_2011.04.28`, the red curve with the new code version `for_2012.11.05f`. Clearly, the large amplitudes and high frequencies are gone and the red curve looks much more like the red curve in Fig. 3, part II of this report, which was obtained with the Roe solver and VanLeer reconstruction.

For both runs, the parameter `s_inflow` = 1.613E+09 and `Teff` = 5000.0. Despite that, the new run does not reach the nominal value for the radiative output but stays at around 0.96, 4% short. This is probably to a large degree due to the fact that the new run has `C_visSmagorinsky` = `C_visArtificial` = 0.0, while in the old run, these values were 1.0 and 0.0, respectively. In fact, comparing run job_d3t50g45mm00n04_f/PP with run job_d3t50g45mm00n04_f/PP_vissmag (see Table 1) we see that the latter has Frtop $\approx 0.98$, which is similar to the values obtained with the Roe solver and VanLeer with the old code (see Fig. 3 of part II).

Figure 8 shows a comparison of the radiative flux for different solvers and reconstruction schemes, all with version `for_2012.11.05f`. The blue curve refers to the run with the Roe solver and VanLeer reconstruction, which used to be our standard combination, which we trust best. All curves show a similar behavior, in particular shows the combination HLLMHD+FRweno a similar behavior as Roe+VanLeer, despite that the two methods are quite different. Here, we see that the model with

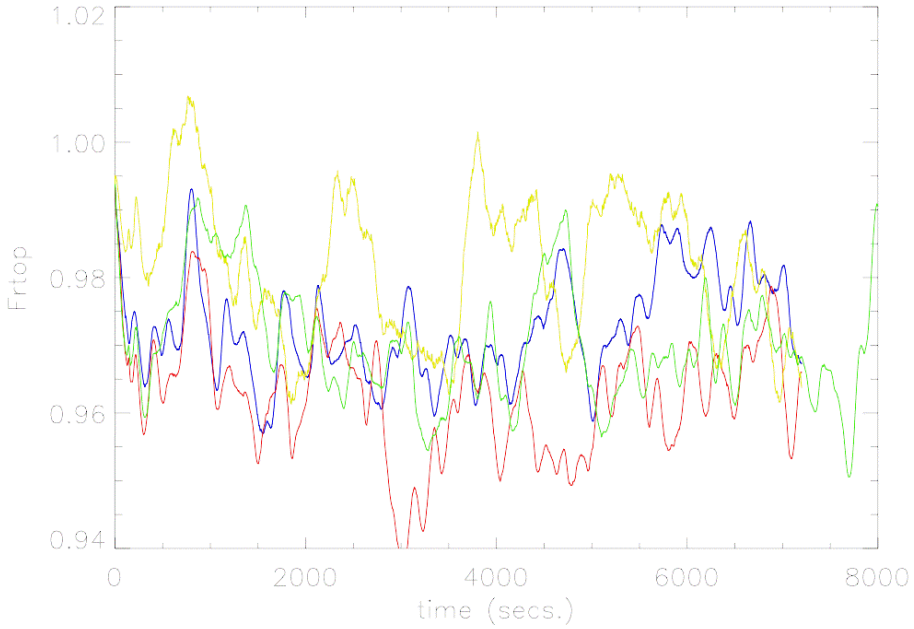


Figure 8: Bolometric radiative flux through the top boundary, Frtop, in units of $\sigma T_{\rm eff}^4$ as a function of time for model d3t50g45mm00n04 with $T_{\rm eff} = 5000$ K and $\mathbf{B} = 0$ or no $\mathbf{B}$ for the run with the Roe solver. All runs with the new code version for_2012.11.05f. *Blue:* Run with the Roe solver and VanLeer reconstruction. *Red:* HLLMHD+PP. *Green:* HLLMHD+FRweno. Yellow: HLLMHD+PP and C_visSmagorinsky = 1.0. All runs with Hancock time integration.

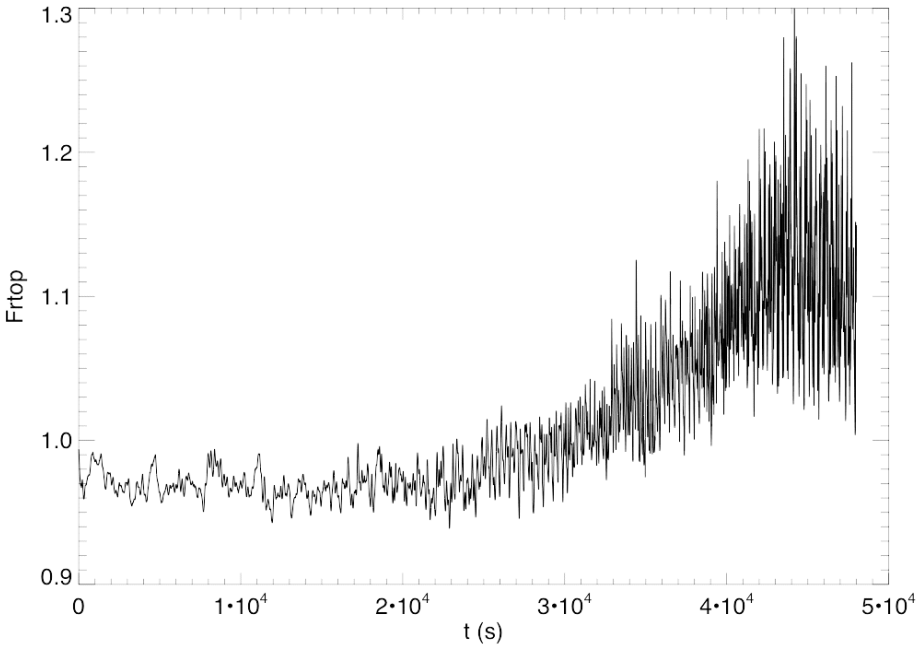


Figure 9: Bolometric radiative flux through the top boundary, Frtop, in units of $\sigma T_{\rm eff}^4$ as a function of time for model d3t50g45mm00n04 with $T_{\rm eff} = 5000$ K and $\mathbf{B} = 0$. Code version for_2012.11.05f, HLLMHD+FRweno and Hancock.

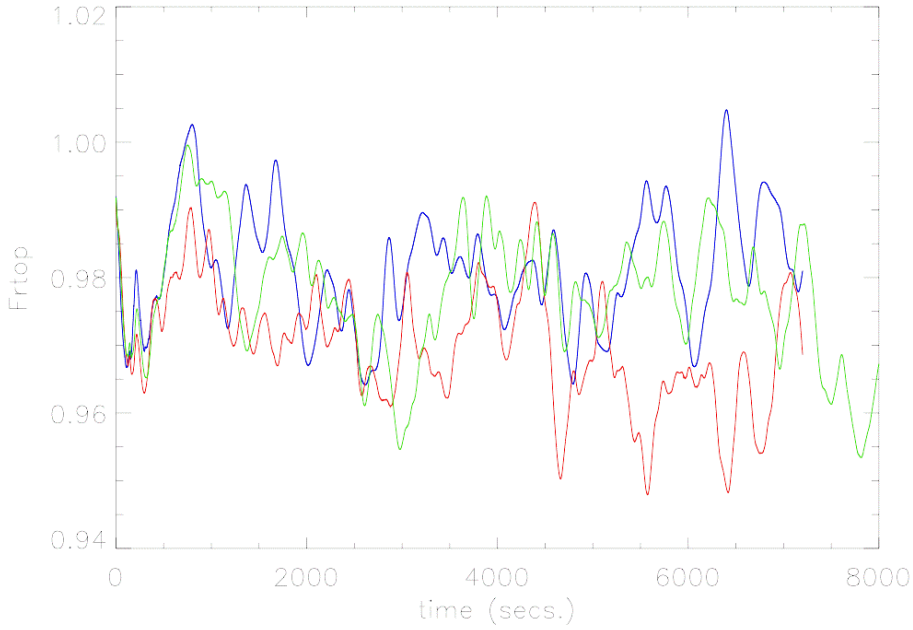


Figure 10: Bolometric radiative flux through the top boundary, Frtop, in units of $\sigma T_{\rm eff}^4$ as a function of time for model d3t50g45mm00n04 with $T_{\rm eff} = 5000$ K and an initial vertical, homogeneous magnetic field of 50 G. All runs with the new code version for_2012.11.05f. *Blue:* Run with the HLLMHD solver and VanLeer reconstruction. *Red:* HLLMHD+PP. *Green:* HLLMHD+FRweno. All runs with Hancock time integration.

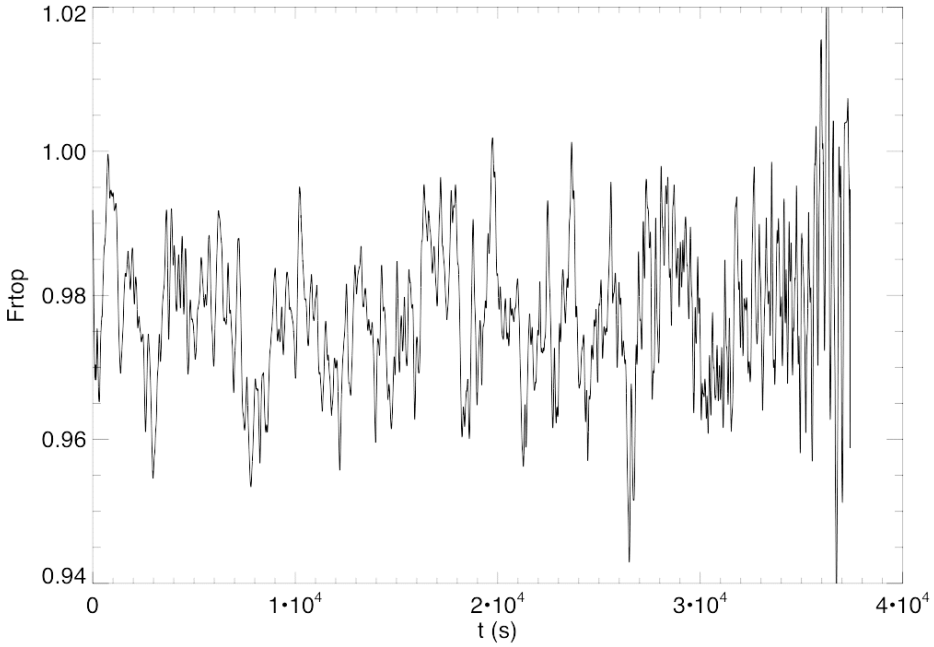


Figure 11: Bolometric radiative flux through the top boundary, Frtop, in units of $\sigma T_{\rm eff}^4$ as a function of time for model d3t50g45mm00n04 with $T_{\rm eff} = 5000$ K and an initial vertical, homogeneous magnetic field of 50 G. Code version for_2012.11.05f, HLLMHD+FRweno and Hancock.

`C_visSmagorinsky` = 1.0 produces the largest flux. This means, that we should slightly adjust `s_inflow` for future simulations with `C_visSmagorinsky` = 0.0. Generally, all curves show a reasonable behavior.

Figure 9 shows the radiative output for the full time span of the run that was carried out with HLLMHD + FRweno and the Hancock time integration with the $T_{\rm eff} = 5000$ K model and with $\mathbf{B} = 0$. This figure can be compared with Fig. 5. Despite the fact that the mass-flux oscillation around $\langle\tau\rangle = 1$ of this model shows a continuously growing amplitude as a function of time (see Fig. 5), the fluctuations in the radiative flux looks inconspicuous over the first about 20'000 s. After that time span however, the radiative output 'explodes'. At this point it is not clear wether this is a consequence of the strongly growing mass flux oscillation or rather vice versa, whether the sudden growth of the radiative throughput has crated the growth in the mass-flux oscillation.

Figure 10 shows a comparison of the radiative flux similar as to Fig. 8 but now for the model with an initial homogeneous vertical magnetic field of 50 G. All curves behave reasonably and they have about half a percent larger flux values than in case of $\mathbf{B} = 0$. Figure 11 shows the full time span for the run with FRweno. Surprisingly, this time the radiative output does not 'explode' despite the fact that the mass-flux amplitude for this model also strongly grows with time as we saw from Fig. 4, which even led to a crash at time $t = 37398$ s. Again, the strong modulation of the mass-flux amplitude of this run (see Fig. 4) does not show up in the radiative flux up to

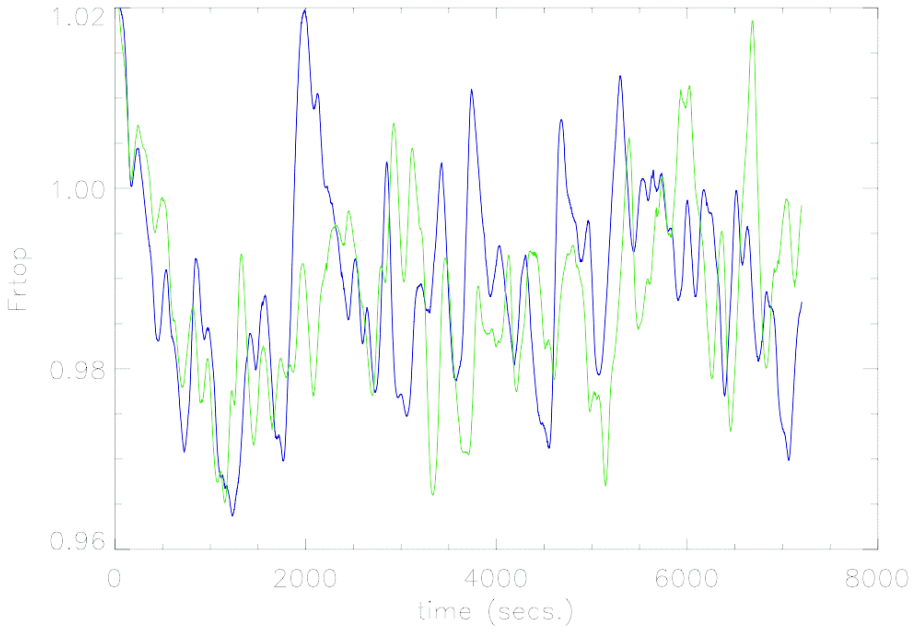


Figure 12: Bolometric radiative flux through the top boundary, Frtop, in units of $\sigma T_{\rm eff}^4$ as a function of time for model d3gt57g44n59 with $T_{\rm eff} = 5770$ K and no magnetic field or $\mathbf{B} = 0$. All runs with the new code version for_2012.11.05f and the Hancock time integration. *Blue:* Roe solver and VanLeer reconstruction. *Green:* HLLMHD+FRweno. All runs with Hancock time integration.

about 30'000 s. After that time, the mass-flux amplitude grows exponentially and that seems to have a response in the radiative flux.

For completeness, we show the radiative output of the solar model `d3gt57g44n59` in Fig. 12, where the blue curve refers to the run with the Roe solver and VanLeer reconstruction (without magnetic field components) and the green curve to the run with HLLMHD and FRweno reconstruction and with $\mathbf{B} = 0$. Again, the two curves look similar without any conspicuousness. This model has not been advanced to longer times so that we don't know if it also starts to 'explode' after a sufficiently long time period.

**Mean vertical mass flux as a function of height**

In part II of this report, we found that the mean vertical mass flux as a function of height $z$, $\langle \rho v_z \rangle (z)$ showed strong wiggles when plotting the cell centred mass flux (`rhov3_xmean`), while the mass flux from the cell interfaces (`rhovb_xmean`) was smooth. This happened only when computing with HLLMHD and PP reconstruction, while Roe+VanLeer as well as HLLMHD+VanLeer showed smooth curves. Therefore, we conjectured that the problem was associated with the PP reconstruction. In this chapter, we revisit this problem and check how the mass fluxes behave when using the FRweno reconstruction scheme.

The first row of Fig. 13 shows the results obtained with the Roe solver combined with the VanLeer reconstruction. Both, the cell centred mass flux (black curve, rhov3_xmean) as well as the mass flux at cell interfaces (red curve, rhovb_xmean) are smooth (except for the lowermost grid cell) and do not strongly deviate from each other. Comparing these plots to Fig. 12 of part II of this report, one should note that the deviation between the two fluxes in the lowermost grid cell is almost an order of magnitude smaller in Fig. 13. Also the HLLMHD solver with VanLeer reconstruction produces smooth fluxes, while the deviation in the lowermost grid cell is larger than with the Roe solver (Fig. 13, second row).

The other curves of Fig. 13 do show wiggles in the cell centered fluxes but they are at least an order of magnitudes smaller than they were with the old code version (compare to Figs. 11 and 14 of part II) and the wiggles straddle the cell-inerface fluxes, so that the deviation between the two fluxes became considerably smaller. Thus, even though it is still not clear why the wiggles in the cell centered fluxes occur with PP and FRweno and not with VanLeer (except of the lowermost few grid points), the problem became less severe. Still, we should keep in mind that the amplitude of the wiggles in the mean mass flux as a function of height is of the same order of magnitude as the amplitude of the mean mass-flux oscillation as a function of time (compare to Figs. 2 to 6). On the other hand, also note that the mass flux at a given location is of the order 1 g $s^{-1}$ $cm^{-2}$, while the wiggle in the mean cell centered mass flux is typically two to three orders of magnitude less.

Fig. 14 shows results similar to Fig. 13 but now for the model with an initial homogeneous, vertical magnetic field of 50 G. The behavior of $\langle \rho v_z \rangle (z)$ is very similar to that of the magnetic filed-free case.

From Fig. 5, we know that the oszillation amplitude of the horizontally averaged, vertical mass flux at the level of $\langle \tau \rangle = 1$ unabatedly increases with time for

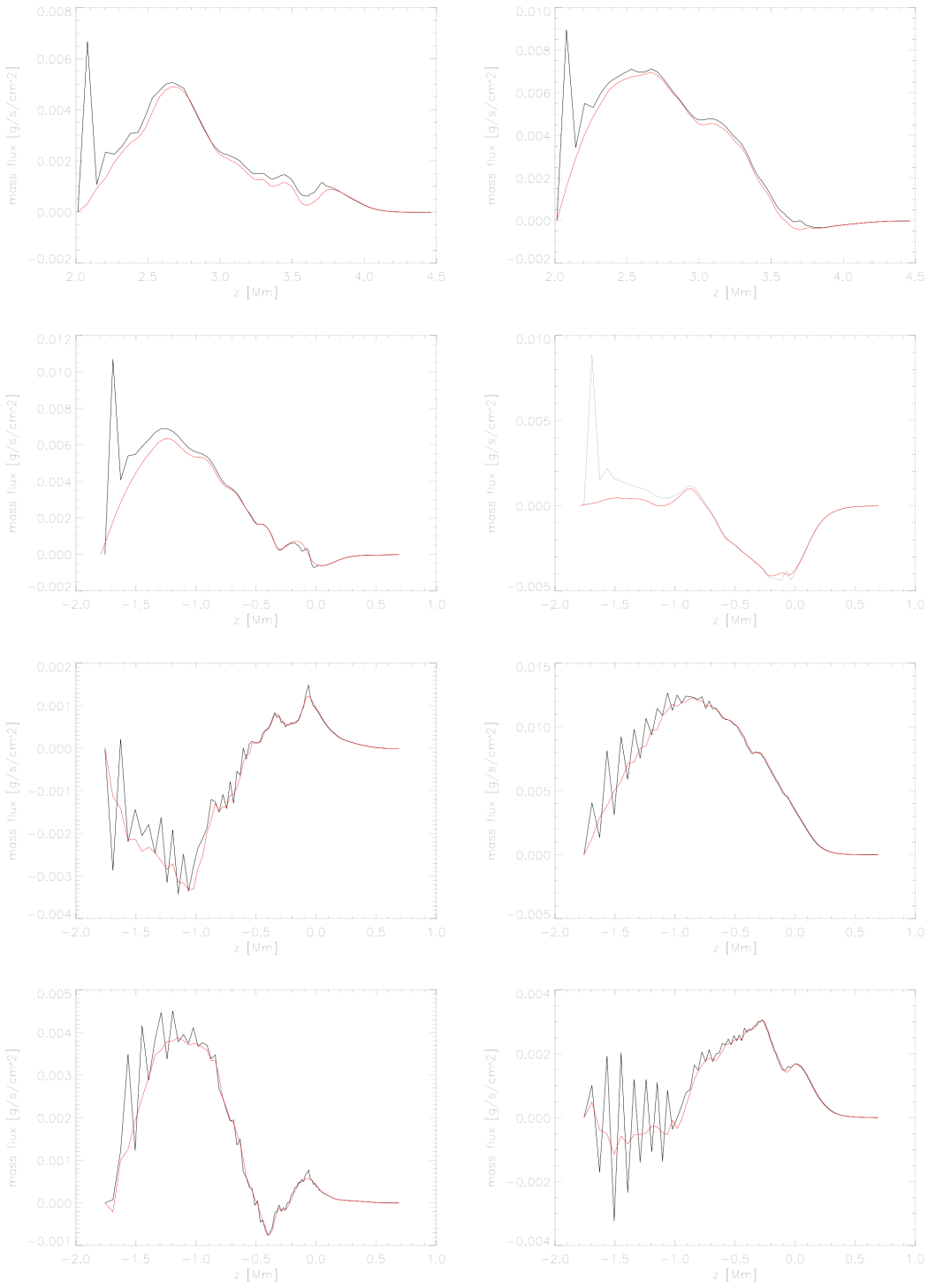


Figure 13: Horizontally averaged, vertical mass flux as a function of height $z$ at time $t = 2420$ s (*left column*) and time $t = 6420$ s (*right column*) for the stellar atmosphere with $T_{\rm eff} = 5000$ K and no magnetic field or $\mathbf{B} = 0$. The *black* curves refer to the cell centred mass flux (rhov3_xmean), the *red* curves to the mass flux at the cell interfaces (rhovb_xmean). *First row:* Simulation with Roe solver and VanLeer reconstruction. *Second row:* HLLMHD and VanLeer. *Third row:* HLLMHD+PP. *Bottom row:* HLLMHD and FRweno.

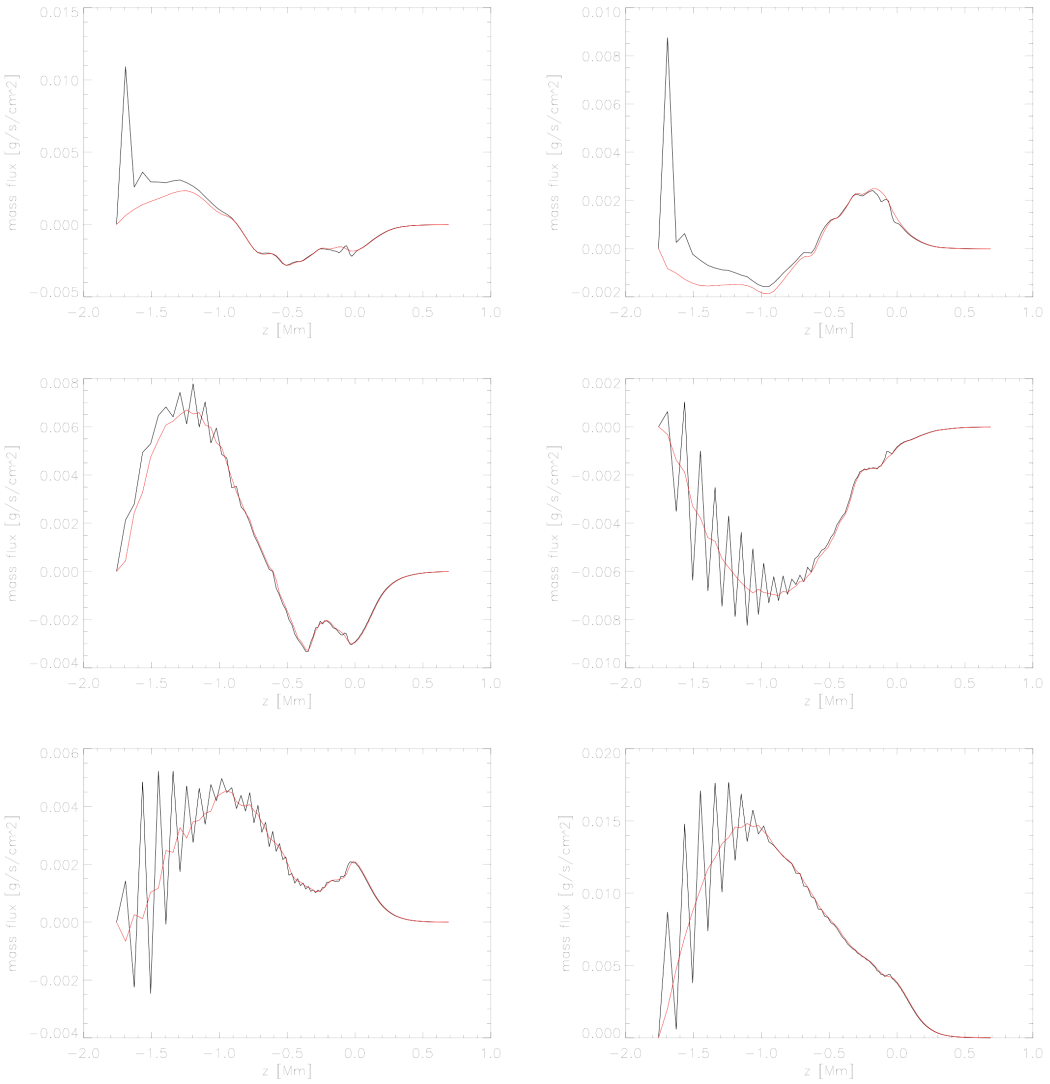


Figure 14: Horizontally averaged, vertical mass flux as a function of height $z$ at time $t = 2420$ s (*left column*) and time $t = 6420$ s (*right column*) for the stellar atmosphere with $T_{\rm eff} = 5000$ K and an initial homogeneous, vertical magnetic field of 50 G. The *black* curves refer to the cell centred mass fluxes (rhov3_xmean), while the *red* curves are the mass fluxes at the cell interfaces (rhovb_xmean). All simulations were carried out with the HLLMHD scheme. *Top row:* Simulation with the VanLeer reconstruction. *Midle row:* Simulation with the PP reconstruction. *Bottom row:* Simulation with the FRweno reconstruction.

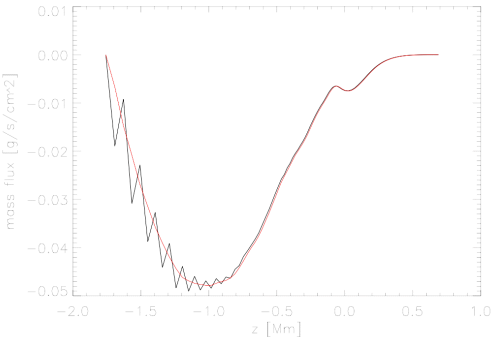


Figure 15: Horizontally averaged, vertical mass flux as a function of height $z$ at time $t = 22420$ s for the stellar atmosphere with $T_{\rm eff} = 5000$ K and $\mathbf{B} = 0$. The *black* curve refer to the cell centred mass flux (rhov3_xmean), the *red* curve to the mass flux at the cell interfaces (rhovb_xmean). The simulation was carried out with the HLLMHD scheme and FRweno reconstruction.

the stellar model with $T_{\rm eff} = 5000$ K and $\mathbf{B} = 0$. Fig. 15 therefore shows the horizontally averaged, vertical mass flux as a function of height $z$ at a much later time, $t = 22420$ s. From this we see that the amplitude of the wiggles does not really grow from $t = 6420$ s (Fig. 13 bottom row, right) to $t = 22420$ s (Fig. 15).

**Experiments with the $T_{\rm eff} = 4000$ K model**

In part III of the present report, we found that the instability that we experienced with the old code version (`for_2011.04.28`) when using HLLMHD and the Hancock time integration was worse with model `d3t40g45mm00n01` than it was with model `d3t50g45mm00n04`, while it was absent with model `d3gt57g44n59`. It looked like the instability became worse with decreasing effective temperature. It is therefore of great interest here to investigate the oscillatory behavior of the $T_{\rm eff} = 4000$ K model as well.

First, we compare the oscillation in radiative flux and mass flux that was obtained with the old code version to the results from the new code version `for_2012.11.05f`. This is done in Figs. 16 and 17 for the first 8000 s—we will later look at at the long term behavior. Clearly, the new code version does much better than the old one in both radiative flux and mass flux. The difference in the level of radiative flux between the red curve (HLL+PP) and the black curve (Roe+FRweno) of about 2% may surprise, but differences can be expected because of the relatively large differences between these two schemes. The curve for Roe+FRweno was omitted in Fig. 17 for clarity, but it has the same amplitude as the red curve (HLLMHD+PP) and looks very similar to the red curve.

Figsures 18 and 19 show a similar comparison as Figs. 16 and 17 but this time all computed with the new code version `for_2012.11.05f`. The blue curve refers to the solution obtained with the Roe solver in combination with FRweno reconstruction, the red curve to the HLLMHD solver in combination with PP reconstruction, and the green curve to HLLMHD+FRweno. The red and green curve of the mass-flux plot

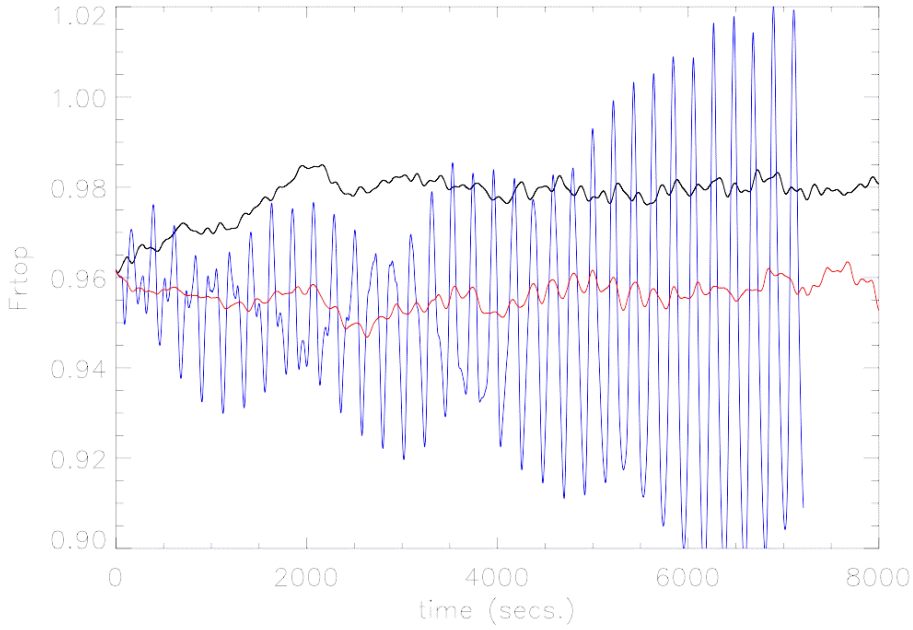


Figure 16: Bolometric radiative flux through the top boundary, Frtop, in units of $\sigma T_{\rm eff}^4$ as a function of time for model d3t40g45mm00n01 with $T_{\rm eff} = 4000$ K and $\mathbf{B} = 0$ or no magnetic field for the run with the Roe solver. *Blue:* Old run with code version for_2011.04.28 using HLLMHD+PP and Hancock time integration. *Red:* New code version for_2012.11.05f using HLLMHD+PP and Hancock time integration. *Black:* New code version using Roe+FRweno and Hancock time integration.

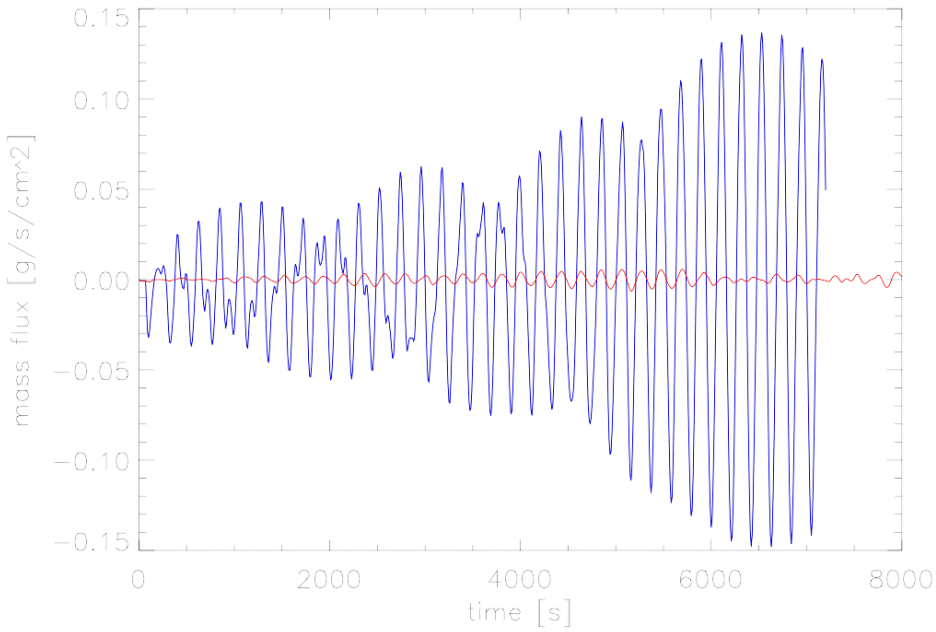


Figure 17: Horizontally averaged, vertical mass flux at the level of $\langle\tau\rangle = 1$ as a function of time for the stellar model with $T_{\rm eff} = 4000$ K and $\mathbf{B} = 0$, computed with HLLMHD and PP, once with the code version for_2011.04.28 (*blue*) and once with the code version for_2012.11.05f (*red*).

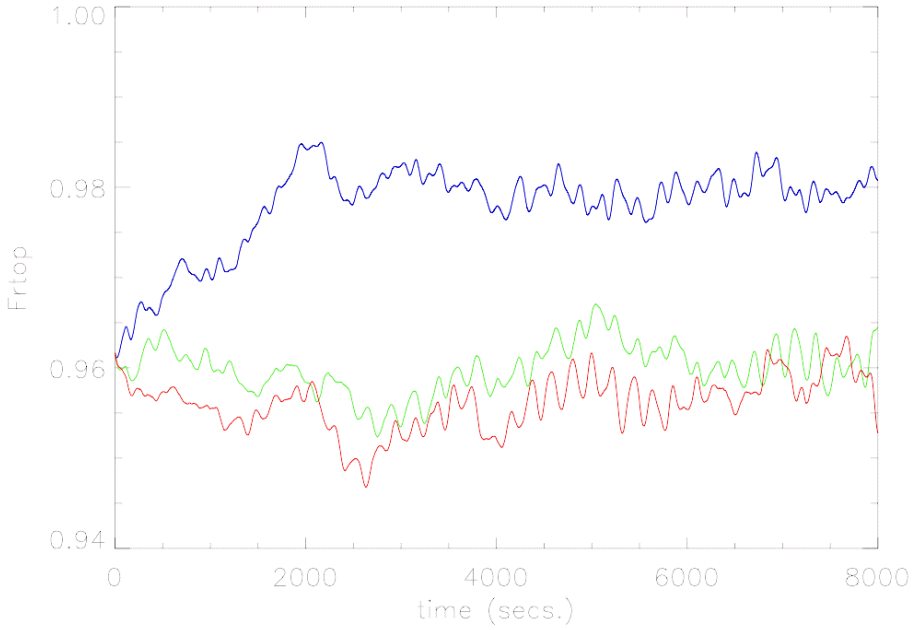


Figure 18: Bolometric radiative flux through the top boundary, Frtop, in units of $\sigma T_{\rm eff}^4$ as a function of time for model d3t40g45mm00n01 with $T_{\rm eff} = 4000$ K and $\mathbf{B} = 0$ or no magnetic field for the run with the Roe solver, all computed with the new code version for_2012.11.05f. *Blue:* Run with the Roe solver and FRweno reconstruction; *Red:* HLLMHD+PP; *Green:* HLLMHD+FRweno.

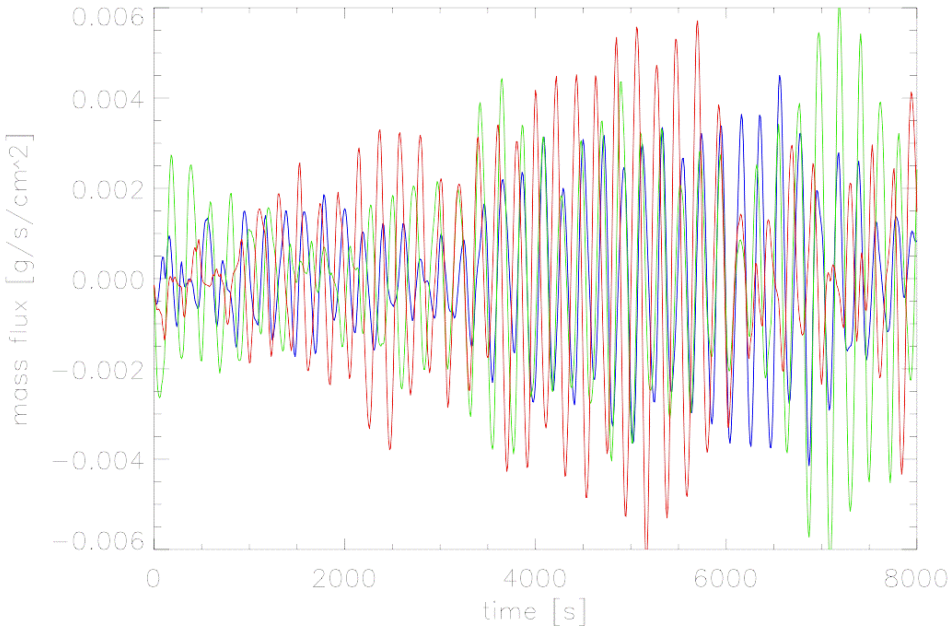


Figure 19: Horizontally averaged, vertical mass flux at the level of $\langle\tau\rangle = 1$ as a function of time for the stellar model with $T_{\rm eff} = 4000$ K and $\mathbf{B} = 0$ or no magnetic field when computed with the Roe solver, all computed with the new code version for_2012.11.05f. *Blue:* Run with the Roe solver and FRweno reconstruction; *Red:* HLLMHD+PP; *Green:* HLLMHD+FRweno.

are very similar and even in phase at later times (not well visible from Fig. 19), which may be attributed to the fact that both are computed using the FRweno reconstruction. From Fig. 18 we see again the difference in flux level between the solution obtained with the Roe solver (blue) and those obtained with the HLLMHD solver (red and green). The red (PP) and green (FRweno) curves are very similar. Note the difference in scales between Figs. 16 and 17, and Figs. 18 and 19.

So far, everything looks fine for the $T_{\rm eff} = 4000$ K model. However, we know from the $T_{\rm eff} = 5000$ K model that the oscillations may grow after a long time, and since our experiences tell us that instabilities worsen with decreasing effective temperature, we also expect this late-time instability to occur for the $T_{\rm eff} = 4000$ K model. This is indeed the case as we can see from the following figures.

Figures 20 and 21 show the oscillation in radiative flux and mass flux up to the time 48 000 s for the model computed with HLLMHD and FRweno. Again, this is for model `d3t40g45mm00n01` with $T_{\rm eff} = 4000$ K and $\mathbf{B} = 0$ and using the code version `for_2012.11.05f`. While the radiative flux 'explodes' only after $\sim 20000$ s, the mass flux shows growing amplitudes from the beginning. When inspecting the models, one finds strong deviation from plane-parallelism at later times when the radiative and mass-flux amplitudes are large, manifest for example in a strongly corrugated $\tau = 1$ surface, much more than is the case for the initial model, when this surface is essentially flat. However, the entropy in the bottom layer has values still very similar to those of the initial model. In any case, the bottom layer does not look very conspicuous other than that the vertical velocity shows a cellular structure of rather mesogranular than granular dimension. I also checked for the total mass in the simulation domain, which I computed by summing `tmpdata.z3.rho_xmean` times the cell hight over all of the x3-axis. There is a decrease of about 4.08 % over the entire time span. However the total mass stays constant to within $6.8 \times 10^{-5}$ within the first half of the time span (24 000 s), which indicates that the mass loss, which becomes drastic after about 30 000 s only, is rather a consequence of the instability than the cause of it. Thus, it does not look like the instability was generated at the bottom boundary or through a continuous mass loss. Comparing Fig. 20 with Fig. 9 and Fig. 21 with Fig. 5 we see indeed that the instability is worse for model `d3t40g45mm00n01` than it was for model `d3t50g45mm00n04` as was expected.

Doing the same plots as Figs. 20 and 21, for an equivalent run but using the PP reconstruction leads to very similar results so that one can say that the instability exists with both the FRweno as well as the PP reconstruction.

Next, I have reduced the radiative Courant numbers: C_radCourant from 2.4 to 0.8 and C_radCourantmax from 2.6 to 1.0 for job FRweno_radc (see Table 1). This had the effect that the time step got partially shortened by more than half of the regular one. However, the result looks very similar as in Figs. 20 and 21. Thus, the instability is not likely due to too large radiative Courant numbers.

In another experiment, I have invoked the point to point viscosity by setting c_visp2pcoeff = 0.2 and c_visp2phypsmagorinsky = 0.2, which are the values now recommended by Bernd Freytag (but for other reasons than suppressing the here discussed instability). Again, the results for the oscillations of the radiative output and the mass flux look very similar to Figs. 20 and 21 so that we can say that the p2p viscosity does not help in suppressing this instability.

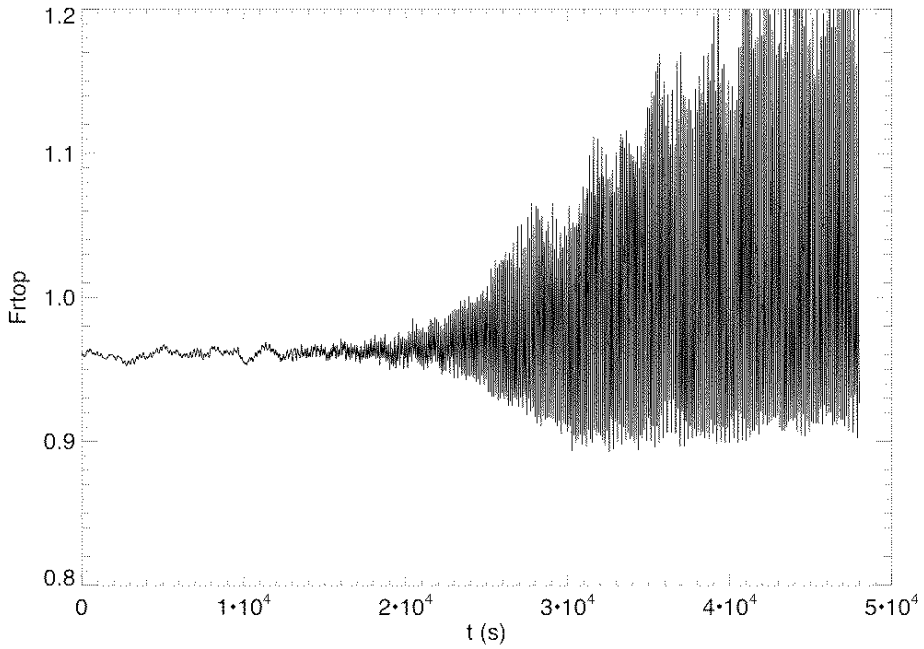


Figure 20: Bolometric radiative flux through the top boundary, Frtop, in units of $\sigma T_{\rm eff}^4$ as a function of time for model d3t40g45mm00n01 with $T_{\rm eff} = 4000$ K and $\mathbf{B} = 0$. Run with the HLLMHD solver and FRweno reconstruction. Code version for_2012.11.05f.

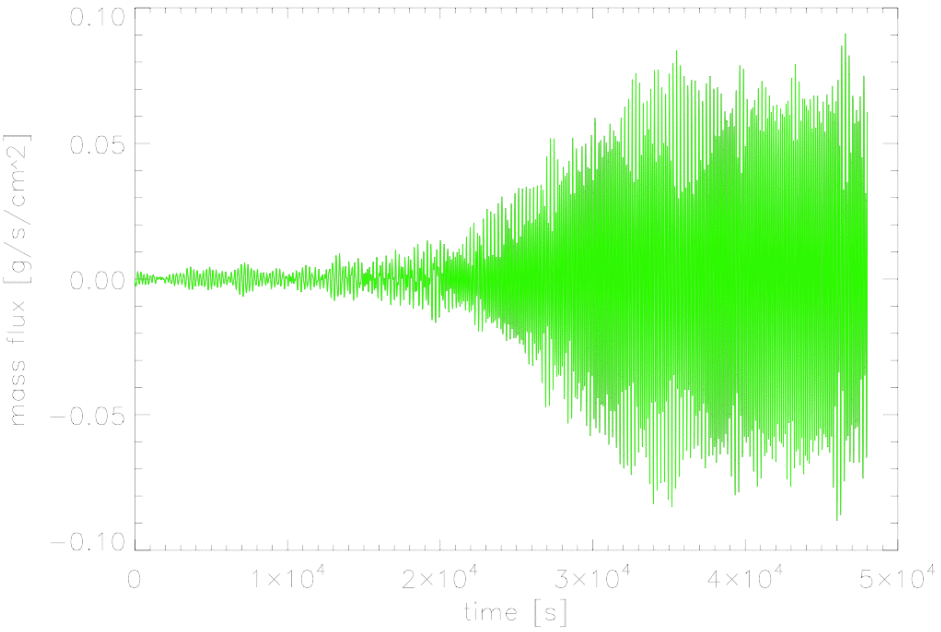


Figure 21: Horizontally averaged, vertical mass flux at the level of $\langle\tau\rangle = 1$ as a function of time for the stellar model with $T_{\rm eff} = 4000$ K and $\mathbf{B} = 0$. Run with the HLLMHD solver and FRweno reconstruction. Code version for_2012.11.05f.

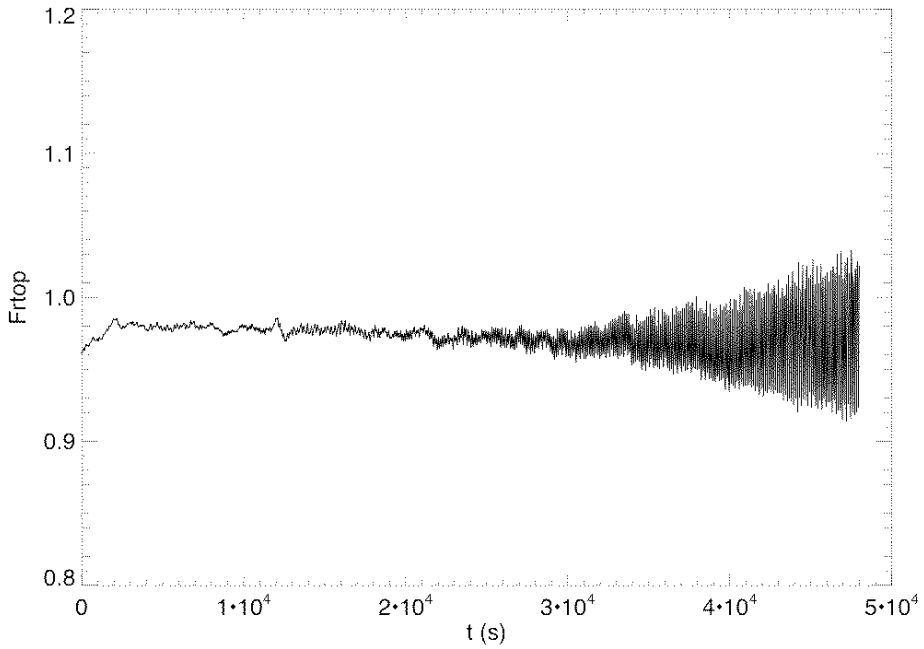


Figure 22: Bolometric radiative flux through the top boundary, Frtop, in units of $\sigma T_{\rm eff}^4$ as a function of time for model d3t40g45mm00n01 with $T_{\rm eff} = 4000$ K and no magnetic field. Run with the Roe solver and FRweno reconstruction. Code version for_2012.11.05f.

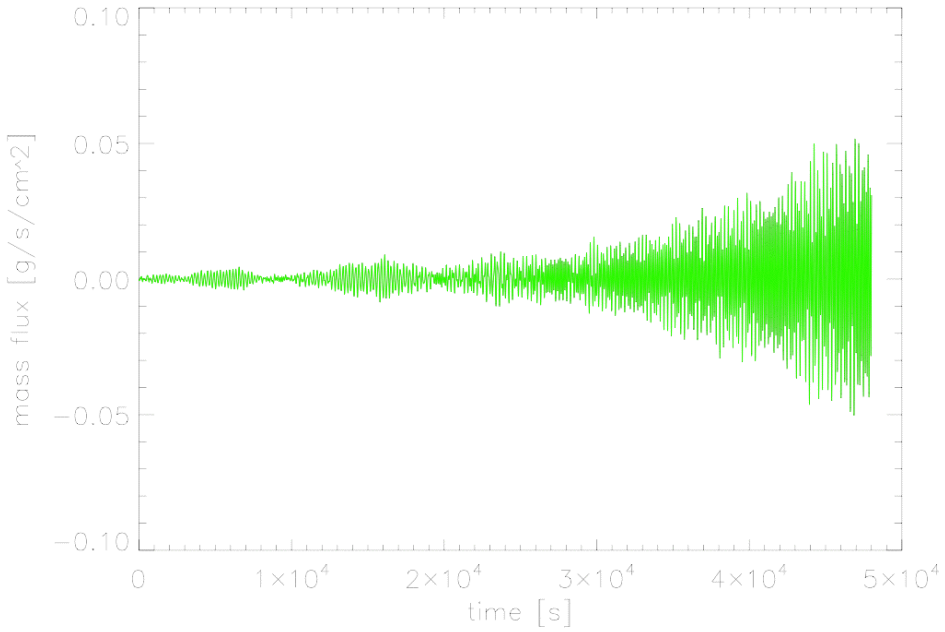


Figure 23: Horizontally averaged, vertical mass flux at the level of $\langle\tau\rangle = 1$ as a function of time for the stellar model with $T_{\rm eff} = 4000$ K and no magnetic field. Run with the Roe solver and FRweno reconstruction. Code version for_2012.11.05f.

Finally, Figs. 22 and 23 show that the instability also occurs when using the Roe solver in combination with the FRweno reconstruction scheme. It is less dramatic than with HLLMHD but also unacceptable. Fig. 21 also nicely shows that the instability seems to exist from the start of the simulation.

**Summary and Conclusions**

Various runs with stellar atmospheres of effective temperatures of 5000 K and 4000 K showed that previously experienced problems when using the Hancock time integration scheme have disappeared with the latest code version `for_2012.11.05f`. The oscillation of the average mass flux trough the height level where $\langle\tau\rangle = 1$ shows normal behavior with Hancock time integration, and irrespective of whether the VanLeer, PP, or FRweno reconstruction scheme was in use. Also, there is no substantial difference in the oscillatory behavior produced by either the Roe solver or the HLL solver.

The same good news can also be reported regarding the radiative flux through the top boundary. Previous spurious oscillations and frequencies with Hancock time integration have disappeared and got replace by normal behavior independent of solver and reconstruction scheme.

Yet another positive news is that the wiggles in the cell-centred average mass flux as a function of height have diminished, while the cell-boundary mass flux as a function of height remains smooth. It is still not understood, why these wiggles occur with PP and FRweno reconstruction but not with VanLeer.

The bad news are that when advancing the simulation for a long duration, we experience a slowly growing instability that leads to unacceptable large oscillations after a time of roughly 20 000 s. This problem was first discovered with the $T_{\rm eff} = 5000$ K model with and without magnetic field, using the HLLMHD solver and FRweno reconstruction. However, it turned out, with the $T_{\rm eff} = 4000$ K model, that it is also present when using the HLLMHD solver in combination with PP and also when using the Roe solver in combination with FRweno. At the beginning, the oscillation amplitude of the average mass flux as a function of time at $\langle\tau\rangle = 1$ shows a modulation on a time scale of roughly 5000 s, but typically grows with each modulation period until to a time of about 20 000 s when it grows very strongly but often to a finite large amplitude only. The radiative output through the top boundary shows inconspicuous behavior during the initial phase of amplitude modulation in mass flux, but then its amplitude starts to grow rapidly, and the average flux grows as well, reaching values of up to 10% above the nominal value. Rather surprisingly, the model with magnetic field did not show this behavior in radiative flux despite that the mass-flux amplitude 'explodes' in this case too. At this stage, I cannot yet tell if this late-time instability also occurs with a solar model and if it was a problem of the Hancock time integration only. Further tests need to be carried out to answer these questions.

Freiburg. i. Br., 16. 8. 2013